An Experimental Study of Emulsion Flow in Alkaline/Solvent Coinjection with Steam for Heavy-Oil/Bitumen Recovery

Kai Sheng, Francisco J. Argüelles-Vivas, Kwang Hoon Baek, and **Ryosuke Okuno,** University of Texas at Austin

Summary

Water is the dominant component in steam-injection processes, such as steam-assisted gravity drainage (SAGD). The central hypothesis in this research is that in-situ oil transport can be enhanced by generating oil-in-water emulsion, where the water-continuous phase acts as an effective oil carrier. As part of the research project, this paper presents an experimental study of how oil-in-water emulsion can improve oil transport in porous media at elevated temperatures.

Diethylamine (DEA) was selected as the organic alkali that generates oil-in-water emulsions with Athabasca bitumen at a 1,000-ppm NaCl brine and a 0.5-wt% alkali concentration. This aqueous composition had been confirmed to be an optimum in terms of oil content in the water-external emulsion phase at a wide range of temperatures. Then, flow experiments with a glass-bead pack were conducted to measure the effective viscosities of emulsion samples at shear rates from 5 to 29 seconds^{-1} at 35 bar and temperatures from 373 to 443 K.

Results show that the oil-in-water emulsions were more than 15 times less viscous than the original bitumen at temperatures from 373 to 443 K. At the shear rate of 5 seconds^{-1}, for example, the emulsion viscosity was 12 cp at 373 K, at which the bitumen viscosity was 206 cp. The efficiency of in-situ bitumen transport was evaluated by calculating the bitumen molar flow rate under gravity drainage with the new experimental data. Results show that oil-in-water emulsion can enhance the in-situ molar flow of bitumen by a factor of 273 at 403 K and 345 at 373 K, in comparison with the two-phase flow of oil and water in conventional SAGD. At 443 K, only a fraction of bitumen is emulsified in water, but the bitumen transport by both oil-in-water emulsion and an excess oil phase in DEA-SAGD can enhance the molar flow of bitumen by a factor of 19 in comparison to SAGD. This is mainly because the mobility of the bitumen-containing phase is enhanced by the reduced viscosity and increased effective permeability. A marked difference between alkaline solvents and conventional hydrocarbon solvents is that only a small amount of an alkaline solvent enables enhancing the in-situ transport of bitumen.

Introduction

SAGD is the in-situ recovery technique widely used for bitumen production. SAGD requires two horizontal wells, several meters apart vertically: The upper well is for steam injection, and the lower well is for production. High-quality steam is injected into the bitumen reservoir and condenses near thermal fronts. The latent heat of the injected water is the main source of energy for reservoir heating. Although only a small fraction of the heat is used for heating bitumen, SAGD effectively reduces the bitumen viscosity owing to high temperature along the edge of a steam chamber.

SAGD needs a large amount of water and energy to generate steam, which makes it a major source of CO_2 emissions (Kim et al. 2017). A cumulative steam/oil ratio, defined as the volume ratio of the injected water (cold-water equivalent) to the produced oil, is an indicator of energy efficiency in steam-based recovery methods. Shen (2013) stated that the cumulative steam/oil ratio has to be controlled to less than 4 m^3/m^3 for an SAGD process to be profitable. To improve the energy efficiency, the coinjection of steam and different solvents has been studied in the literature, such as *n*-alkanes and condensates (Nasr et al. 2003; Gates 2007; Ivory et al. 2008; Li et al. 2011a, 2011b; Keshavarz et al. 2014, 2015).

Investigations into solvent-SAGD phase behavior have shown that, in general, these processes perform better in terms of production rate as the carbon number of the injected solvent increases (Li et al. 2011a; Mohebati et al. 2012; Keshavarz et al. 2015). Pilot tests, such as EnCana's solvent aided process (SAP) pilot and Imperial Oil's liquid addition to steam for enhancing recovery (LASER), have demonstrated the potential of hydrocarbon solvent and steam coinjection to improve the bitumen recovery and reduce the cumulative steam/oil ratio (Leaute 2002; Nasr et al. 2003; Gupta et al. 2005; Gupta and Gittins 2006; Gates 2007; Leaute and Carey 2007; Li et al. 2011a, 2011b; Keshavarz et al. 2014, 2015). However, the economic feasibility of solvent-SAGD can be highly uncertain when a substantial amount of the cost is associated with the injected solvent and its treatment for recycling. Efficient use of the solvent is important for a solvent process to be economically successful.

Recently, Sheng et al. (2018) showed that water, the dominant component in the SAGD process, can be used as a solvent carrier to improve the efficiency of SAGD. They conducted a numerical simulation study of dimethyl ether (DME), a water-soluble solvent. In their simulations, DME-SAGD was able to achieve a 40% lower cumulative steam/oil ratio and a 24% faster bitumen drainage at an early stage of coinjection than SAGD, and a 20% greater solvent recovery than *n*-butane-SAGD, as a result of DME's solubility in both water and bitumen. Other researchers have also studied phase behavior and thermophysical properties of mixtures of bitumen and DME (Baek et al. 2019a; Haddadnia et al. 2018). In these studies, DME was used as a viscosity reducer for bitumen and heavy oil.

All methods mentioned above depend mainly on viscosity reduction by temperature and/or by dilution by a condensed solvent near the edge of the steam chamber. However, it is also possible to enhance in-situ bitumen transport by making oil-in-water emulsions, where the water-external phase acts as an effective carrier of bitumen even at low temperatures. One way to make such emulsions is to activate acidic components in the in-situ bitumen as natural surfactants by adding organic alkali to steam. Baek et al. (2018a, 2018b) reported that Athabasca bitumen could be completely emulsified in water at low salinities (<1,000 ppm) and low alkali concentrations in brine (<5 wt%) at temperatures up to 373 K at atmospheric pressure. The low concentration of alkali required to emulsify bitumen is advantageous because the project's economics would be less affected by reservoir uncertainties.

This paper (SPE 190224) was accepted for presentation at the SPE Improved Oil Recovery Conference, Tulsa, Oklahoma, USA, 14–18 April 2018, and revised for publication. Original manuscript received for review 17 November 2018. Revised manuscript received for review 14 July 2019. Paper peer approved 15 July 2019.

The use of alkali has been studied for heavy-oil reservoirs in which steam injection is not an attractive option. Waterflooding processes such as alkaline flooding, alkaline and surfactant, alkali and polymer, and alkali/cosolvent/polymer have the purpose of achieving an ultralow interfacial tension, emulsification, and transport of heavy oil in water, and/or improvement of sweep efficiency through water-in-oil or oil-in-water emulsions (Liu et al. 2006; Bryan and Kantzas 2007a, 2007b; Liu et al. 2007; Bryan et al. 2008; Dong et al. 2009; Kumar et al. 2012; Pei et al. 2013; Fortenberry et al. 2015; Xiao et al. 2017).

Some attempts have also been made to emulsify heavy oil and bitumen in water through steam/surfactant coinjection. Zeidani and Gupta (2013) and Lu et al. (2017) used commercially available surfactants with strong hydrophilicity to generate oil-in-water emulsions to improve bitumen recovery. Srivastava and Castro (2011) applied a class of surfactants called thin-film-spreading agents to enhance the cyclic-steam-stimulation method in Canadian heavy-oil reservoirs.

Only two studies focused on alkalis as additives to steam for SAGD. Kim et al. (2017) studied an alkaline-based SAGD process in a micromodel to explain recovery mechanisms at the pore scale. They found that the emulsification of bitumen into water and the alteration of wettability toward a water-wet state were the mechanisms that enhanced bitumen recovery. Baek et al. (2018a) demonstrated that a small amount of organic alkali, DEA, can form oil-in-water emulsions when mixed with brine and bitumen. Their phase behavior study showed that low alkali concentrations and salinity less than 1,000 ppm are favorable conditions to form a single phase of oil-in-water emulsion. Baek et al. (2018a) also showed that, in comparison with bitumen, these emulsions were three to four orders of magnitude less viscous at 298 K and two orders of magnitude less viscous at 323 K.

However, no research has been conducted on the capability of oil-in-water emulsion as a bitumen carrier in porous media. The objective of this research is to determine the rheological properties of oil-in-water emulsions for their role as bitumen carriers in porous media, by adding DEA to Athabasca bitumen and a 1,000-ppm NaCl brine. The concentration of DEA in the brine was set to 0.5 wt% on the basis of the phase-behavior study of Baek et al. (2018a). The main novelty of this research lies in the new experimental data for emulsion phase behavior and rheological properties at 35 bar and temperatures up to 443 K. The results are used to analyze the bitumen molar flow rates under gravity drainage for oil-in-water emulsions (DEA-SAGD) and the two-phase flow of oil and water (conventional SAGD).

In what follows, the Experimental Materials and Methods section introduces the experimental materials and methods of phase-behavior tests, density measurements, and effective viscosities in a porous medium. The Results and Discussion section presents the experimental results and detailed analysis of them on the basis of a gravity-drainage equation.

Experimental Materials and Methods

This section presents the materials, apparatus, and procedures used for the experimental part of this research.

Materials. A dehydrated Athabasca bitumen sample was used for this research and was analyzed by a commercial laboratory (Exova laboratory, Edmonton, Alberta, Canada). The molecular weight was measured to be 532 g/mol by a freezing-point-depression method. Compositional analysis showed 24.5 wt% saturates, 36.6 wt% aromatics, 21.1 wt% resin, and 17.8 wt% asphaltenes (pentane-insoluble). The density of the bitumen was 0.985 g/cm^3 at 335 K and atmospheric pressure. The total acid number of the bitumen sample was measured to be 3.56 mg KOH/g oil, using the method of Fan and Buckley (2007). This acid number indicates that bitumen contains a significant amount of acidic components, which can be activated as natural surfactants in a high-pH aqueous solution.

In this research, oil-in-water emulsions were prepared by mixing the bitumen sample with an aqueous solution with 0.5 wt% of DEA and 1,000 ppm of NaCl. That is, this experiment was conducted under the assumption that the coinjection of steam with DEA resulted in 0.5 wt% DEA in a 1,000 ppm NaCl brine near the steam chamber edge. The brine was made with deionized water. The DEA was provided by Sigma-Aldrich, with a purity of 99.5%. The pH of the aqueous solution with 0.5% DEA and 1,000 ppm of NaCl was measured to be 10.48.

DEA has the chemical formula of $(CH_3CH_2)_2NH$ and a molecular weight of 73 g/mol. DEA was selected as the organic alkali in Baek et al. (2018a) and in this research, primarily because the volatility of DEA is between n-C_5 and n-C_6. DEA is expected to propagate in the reservoir as part of the vapor phase and to condense at thermal fronts.

Approximately 70 cm^3 of a brine/DEA/bitumen mixture was prepared for the density and phase-behavior measurements and the emulsion-flow tests in a glass-bead pack. An aqueous solution of 0.5 wt% DEA and 1,000 ppm NaCl was prepared first. Then, this solution was mixed with the bitumen at the volume ratio of 7:3 at atmospheric pressure and 296 K. The mixture was sealed and heated to 353 K and then stirred for 1 day with a magnetic stirrer on a stirring heating plate at a speed of no more than 500 rev/min. The mixture was left for an additional 2 days in the accumulator before it was injected into the density meter or the glass-bead pack, as will be shown in the following subsections.

In solvent-SAGD, it is expected that the injected solvent is condensed and mixed with bitumen near the edge of the steam chamber mainly through transverse dispersion (Keshavarz et al. 2015; Meng et al. 2018). The experimental study of Meng et al. (2018) confirmed that the mixing was enhanced by convection (i.e., dispersion) between bitumen and solvent in solvent-SAGD. Likewise, it is expected that DEA is condensed and mixed with water and oil near the edge of the steam chamber through transverse dispersion in DEA-SAGD. When acidic oil components are in contact with a DEA solution, bitumen is emulsified with water by the natural surfactants generated. **Fig. 1** is a schematic that illustrates the condensation and mixing of DEA with water and bitumen near the edge of the steam chamber.

As described in the Introduction section, the focus of this research is on bitumen transport when bitumen is emulsified in water by a small amount of DEA. How DEA is going to mix with water and bitumen at an elevated temperature in porous media during DEA-SAGD is an open question and beyond the scope of the current paper.

Emulsion Density and Phase-Behavior Measurements. Baek et al. (2018a) studied the phase behavior of the same mixture (30 vol% Athabasca bitumen + 70 vol% aqueous solution of 0.5 wt% DEA and 1,000 ppm NaCl) at atmospheric pressure and temperatures up to 373 K as part of their research. The pressure and temperature conditions in Baek et al. (2018a) were limited because glass pipettes were used for a more general observation of phase behavior. In this research, the phase behavior of this specific mixture was studied at 373, 403, and 443 K at 35 bar, which are conditions more representative of SAGD operations.

Phase densities were measured by an in-line densitometer (Anton Paar, Graz, Austria) for this mixture. In-line density measurement also enables detection of any phase boundary, and phase amounts at these high-temperature/high-pressure conditions without direct visual observation. Measured data will be used to analyze the bitumen transport by oil-in-water emulsion in a later section.

Fig. 2 shows the setup for density and phase-behavior measurements for water/bitumen/DEA emulsions. The setup consists of two pumps, two accumulators, an in-line density meter, a pressure gauge, and an oven. One accumulator was used for the mixture to be injected, and the other for the effluent side of the density meter. An Omega pressure gauge (model PX459-2.5KGI-EH), located close to the inlet of the density meter, was used to measure the absolute pressure of the system.

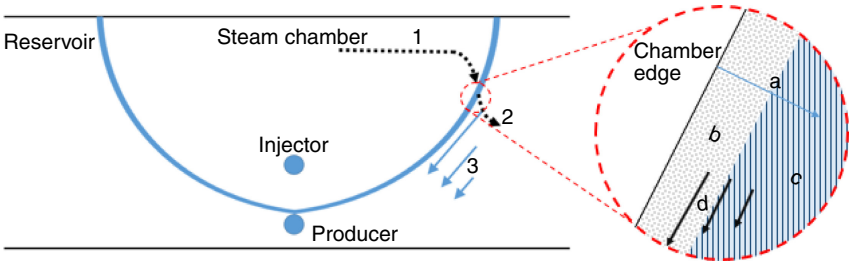

1—Steam and DEA gradually condense as they propagate inside the chamber until the vapor phase disappears at the chamber edge.
2—Condensed water and DEA (a high-pH aqueous phase) are in contact with mobile bitumen and connate water; then, bitumen is emulsified by natural surfactants generated by the reaction of DEA with naphthenic acids.
3—Emulsion, bitumen, and water flow downward under gravity.
a—Condensed DEA is dispersed through the aqueous phase.
b—Dispersed DEA reacts with acidic bitumen components. The generated natural surfactants yield oil-in-water emulsion.
c—Bitumen that is present beyond the DEA dispersion fronts has not been emulsified, and may or may not flow, depending on its mobility.
d—Emulsion, bitumen, and water flow as multiphase flow under gravity.

Fig. 1—Schematic of DEA condensation and mixing with water and bitumen near the edge of a chamber. This schematic is not drawn to scale and is added merely for the purpose of qualitative explanation of DEA-SAGD.

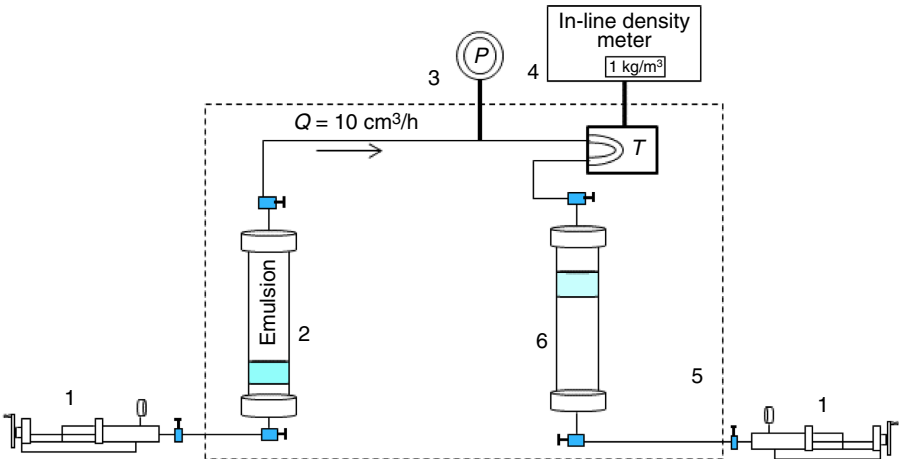

1. Pressurization pump
2. Sample accumulator
3. Pressure gauge
4. In-line density meter
5. Oven
6. Effluent collector

Fig. 2—Schematic of the experimental setup for measuring density and for detecting phases for water/bitumen/DEA mixtures.

The fluid sample passes through a measuring cell that uses a U-shaped tube where the fluid density is measured. This density meter is capable of measuring fluid densities from 0 to 3000 kg/m^3 with an instrument precision of ±1 kg/m^3. A Despatch oven (LAC2-18-8) was used to heat up the system and to control the temperature. A monitor outside the oven is connected to the in-line density meter to display the measured density, pressure, and temperature. The manufacturers' instrument precisions of the temperature and pressure gauges are ±0.1°C and ±0.08% best-straight line, respectively.

Before each measurement, the in-line density-measurement system was cleaned meticulously with a 50:50 vol% methanol/toluene mixture, dried with nitrogen, and evacuated for at least 2 hours. Then, the system was filled with helium at 35 bar using the effluent accumulator (Number 6 in Fig. 2).

The pressure of the system was maintained through the effluent accumulator with an Isco pump that was operated at the constant pressure mode during all experiments. To ensure that there were no leakages in the setup, the pressure was monitored at least for 5 hours. Next, the accumulator containing 70 cm^3 of a water/bitumen/DEA emulsion (previously aged at 353 K for 2 days in the same oven) was promptly connected to the in-line system through its upper valve and pressurized to 35 bar. Then, the oven was heated to a test temperature (373, 403, or 443 K). Once the system temperature stabilized, the upper valve of the emulsion accumulator was open. Then, the Isco pump controlling the same accumulator was switched to the constant-flow-rate mode. The flow rate was set to 10 cm^3/h, and the helium was displaced from the system and collected in the effluent accumulator.

The density of the flowing fluid was recorded every second the mixture reached the density meter. If there was a change in density, indicating a phase boundary, the sample was collected for compositional analysis. For such a case, a new accumulator for storing the effluent was connected to the system, and the experiment was restarted to measure the density of the remaining sample.

Flow of Bitumen and Oil-in-Water Emulsion Through a Porous Medium. Effective viscosities for oil-in-water emulsions at different shear rates and bitumen viscosities were measured through glass-bead packs. Measurement of the effective viscosity of emulsions is

performed on the basis of Sadowski and Bird (1965), who used a generalized Darcy's law for Newtonian and non-Newtonian fluids. Brine is a Newtonian fluid, and oil-in-water emulsion is generally a non-Newtonian fluid. Assuming the same interstitial structures, permeability, porosity, cross-sectional area, and length, the effective viscosity of the emulsion can be determined by

$$\mu_{\text{emulsion}} = \frac{\Delta P_{\text{emulsion}}}{\Delta P_{\text{brine}}} \mu_{\text{brine}}, \quad (1)$$

where μ is the viscosity and ΔP is the pressure drop. Note that the emulsion viscosities so determined are "effective" values under the measured $\Delta P_{\text{emulsion}}$ because all other parameters are assumed unchanged in comparison with brine flow.

Fig. 3 shows the setup for the corefiooding tests. This coreflooding setup consists of two pumps, four accumulators, a glass-bead pack, a pressure transducer, an absolute-pressure gauge, and a temperature gauge. A glass-bead pack was placed horizontally inside the oven. The glass-bead holder is a 0.25-in. (outer-diameter) stainless-steel tube with a length of 0.5 m. The volume inside the tube is 8.2 cm^3. The pressure drop along the porous medium was recorded by an Emerson differential-pressure transducer. The pressure transducer is capable of measuring pressure drops from 0 to 2.1 bar with an instrument precision of 0.001 bar. A thermometer (RTD model PR-11-2-100-one-eighth-12-E) was placed near the inlet of the glass-bead pack to monitor the temperature of the oil-in-water emulsions.

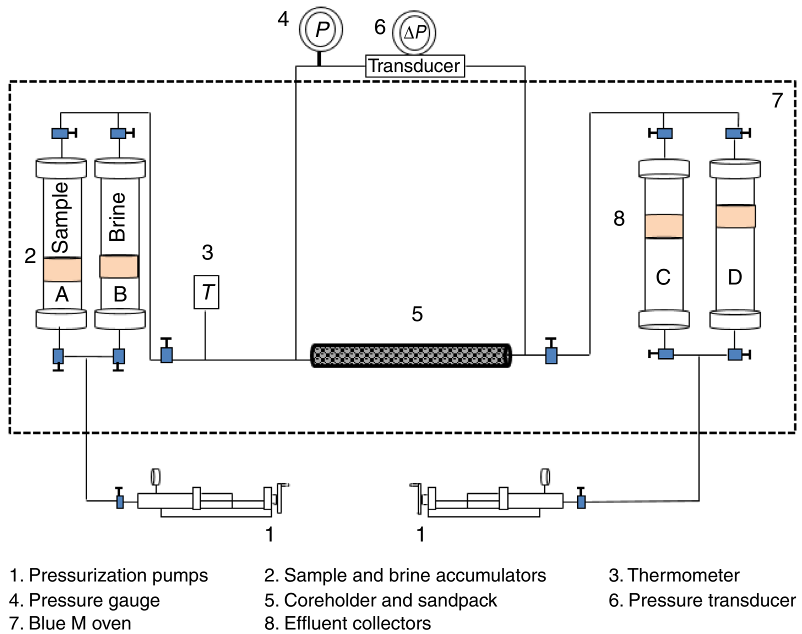

Fig. 3—Schematic of the experimental setup for measuring effective viscosities of oil-in-water emulsion and bitumen viscosities with a glass-bead pack.

The porous medium for the measurement of effective viscosities for oil-in-water emulsion inside the pipe is a reproduction of a fine-grained oil sand sample from the Middle McMurray Formation (Athabasca, Alberta, Canada) (Mohammadmoradi et al. 2017), which is a major bitumen-production zone. The porous medium is a glass-bead pack with particle diameters ranging from 63 to 500 μm, with a median diameter of 169 μm. The two ends were covered by stainless-steel screens with an opening size of 53 μm to prevent bead production and the crumbling of the pack during the emulsion flow tests. The porosity and absolute permeability of the sandpack were measured with brine at 373, 403, and 443 K and 35 bar several times. The resulting porosity and permeability were on average 35% and 11.6 darcies, respectively, and were not sensitive to temperature.

Two accumulators (A and B in Fig. 3) containing the brine and water/bitumen/DEA emulsion, respectively, were placed inside the oven, connected to the experimental setup and pressurized to 35 bar. Two more accumulators (C and D in Fig. 3) for 50 cm^3 of distilled water were connected on the downstream side of the outlet valve of the glass-bead holder to store the effluent and hold the pressure of the experiments. Accumulators C and D operated at a constant backward flow rate during the flow tests. The oven was heating to the temperature of the test, and the setup was evacuated for at least 4 hours, including the tubings and the glass-bead pack. Once the test temperature became stable, the upper valve of the brine accumulator was opened to saturate the system with brine. The porosity of the glass-bead pack was calculated. Then, the pump that controlled the brine accumulator was switched to the constant-flow-rate mode. After that, the outlet valve of the glass-bead pack and the valve of Accumulator C were opened. The pressure drop along the bead pack was recorded, and the brine was collected in Accumulator C.

The brine accumulator was isolated after measuring the porosity and absolute permeability. The pump controlling the emulsion accumulator was switched to a constant flow rate to displace the brine and saturate the glass-bead pack with the water/bitumen/DEA emulsion. Once the glass-bead pack was saturated by the emulsion, the pressure drop was measured to obtain an effective viscosity of emulsion. Accumulator D was used to store the water/bitumen/DEA emulsion on the effluent side.

Before starting a new experiment, the system was cleaned thoroughly with a 50:50 vol% methanol/toluene mixture until the initial porosity and absolute permeability were restored. Then, the system was dried in a vacuum. The effective viscosities of emulsions were obtained at 373, 403, and 443 K at 35 bar and different shear rates.

The measurement of bitumen viscosity used the same setup as shown in Fig. 3 but with a different glass-bead pack. The use of a different porous medium does not affect the viscosity measurement because the dehydrated bitumen is a Newtonian fluid. The measurement was validated with the viscosities independently measured for the same bitumen by Baek et al. (2018a) using a rheometer.

The porous medium used for the bitumen viscosity measurement is a glass-bead pack with particle diameters ranging from 250 to 425 μm. The two ends were covered by stainless-steel screens with an opening size of 53 μm to prevent bead production. The resulting absolute permeability of the sandpack was measured to be 90.5 darcies and was not sensitive to temperature according to multiple measurements from 373 to 443 K at 35 bar. Bitumen viscosities were measured at 373, 403, and 443 K and 35 bar.

Results and Discussion

Density Measurement and Phase Behavior. **Fig. 4** shows the measured densities at 35 bar and 373, 403, and 443 K. The horizontal axis is a dimensionless cumulative volume, defined as the cumulative injected volume divided by the total volume of the water/bitumen/DEA mixture. This axis represents the volumetric fraction injected (i.e., if two phases are present, the point at which a change in density is observed represents the phase-volume fraction of the less-dense phase). **Table 1** shows the measured emulsion densities along with the densities of water and bitumen taken from the National Institute of Standards and Technology (NIST)[*] and Baek et al. (2019a). The bitumen used by Baek et al. (2019a) and in this research is denser than water by 2.6, 7.6, and 20.4 kg/m^3 at 373, 403, and 443 K, respectively.

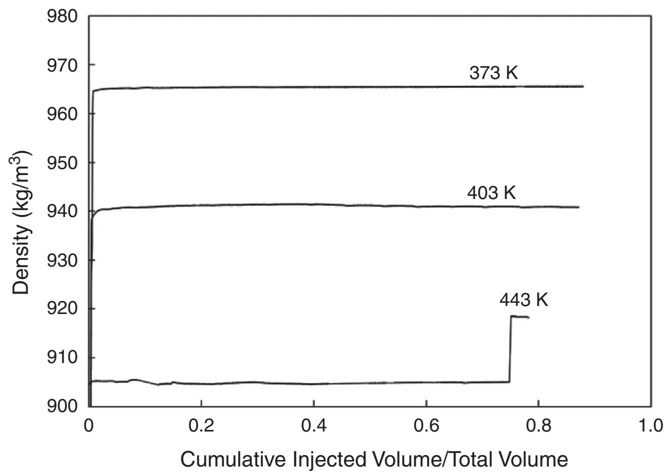

Fig. 4—Measured densities are presented with respect to dimensionless cumulative injected volume at 35 bar and 373, 403, and 443 K. The dimensionless cumulative injected volume is defined as the cumulative injected volume divided by the total volume. There is only a single-phase emulsion at 373 and 403 K.

	373 K	403 K	443 K	
Phase identity	Emulsion	Emulsion	Emulsion	Oil
Average emulsion density	965.5	941.1	904.8	918.1
Water (NIST)[*]	959.9	936.8	899.4	
Bitumen (Baek et al. 2019a)	962.3	944.2	919.7	

Table 1—Water, bitumen, and emulsion densities (kg/m^3) measured at 35 bar and 373, 403, and 443 K.

Fig. 4 presents that the mixture formed a single-phase emulsion at 373 and 403 K at 35 bar. All the bitumen was emulsified within the water continuous phase. Single-phase water-external emulsions for the same mixture were also observed at atmospheric pressure at temperatures up to 373 K in Baek et al. (2018a). The emulsion density measured at 373 K was approximately 3 kg/m^3 greater than the bitumen density calculated at 373 K by the density model for the same Athabasca bitumen sample (Baek et al. 2019a). Although the bitumen samples used in this research and in Baek et al. (2019a) were taken from the same 5-gal container, this unexpected result might be attributed to some nonhomogeneity of bitumen composition inside the container at room temperature.

At 403 K, the emulsion density was between water and bitumen densities. A single-phase oil-in-water emulsion is expected to contribute to enhancing in-situ bitumen transport by increasing the effective permeability to the highly mobile water phase that contains bitumen.

Two phases were detected at 443 K. The first phase represented 74.7 vol%, which was observed to be an oil-in-water emulsion at room temperature and atmospheric pressure. The second phase was a bitumen-rich phase (918.1 kg/m^3), as indicated by the densities of bitumen (919.7 kg/m^3) at 443 K and 35 bar. Visual inspection at room temperature indicated that the second phase was a bitumen-rich phase with dissolved or dispersed water. Composition analysis showed that the first phase contained approximately 12 vol% (0.47 mol%) of bitumen and the second phase approximately 85 vol% (16.2 mol%) of bitumen. This small amount of bitumen-in-water emulsification can be significant in terms of the in-situ bitumen transport in DEA-SAGD, as will be discussed later.

Bitumen Viscosity and Effective Viscosity of Emulsion. The bitumen viscosity was measured to be 205.6, 58.2, and 18.4 cp at 373, 403, and 443 K at 35 bar, respectively. **Fig. 5 and Table 2** show the effective-viscosity data for the emulsion at 373, 403, and 443 K at 35 bar. Following Lake et al. (2014), the equivalent shear rate ($\dot{\gamma}_{eq}$) in a porous medium can be estimated by

$$\dot{\gamma}_{eq} = \frac{4q}{A\sqrt{8k\phi}}, \quad (2)$$

[*]NIST Reference Fluid Thermodynamic and Transport Properties Database (NIST REFPREP) version 7. https://webbook.nist.gov/chemistry/fluid/.

where q is the Darcy flow rate in cm^3/s, A is the cross-sectional area of the core in cm^2, k is the permeability in cm^2, and ϕ is the porosity. At 373 K, the emulsion showed a slightly shear-thinning behavior at shear rates from 5 to 29 $seconds^{-1}$. The emulsion viscosity at 403 K is 2–3 times lower than that at 373 K. At 403 and 443 K, the emulsion viscosity did not show a clear sensitivity to shear rate from 5 to 29 $seconds^{-1}$. The effective viscosity of emulsion is 20 times lower than the bitumen viscosity at 373 K, 15 times at 403 K, and 19 times at 443 K. Note again that the bitumen content in the emulsion at 443 K is 3 times lower than those at 373 K and 403 K, which largely explains why the emulsion viscosity at 443 K is approximately 4 and 10 times lower than those at 373 K and 403 K (Fig. 5b). An average effective viscosity is taken from the data between 5 and 10 $seconds^{-1}$ at each temperature and used for calculating the molar flow rates of bitumen in the next subsection.

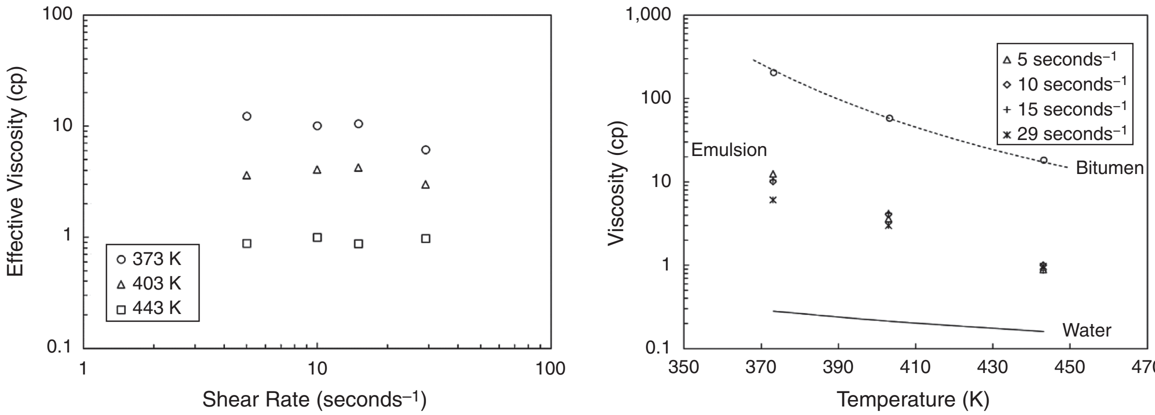

(a) Effective emulsion viscosity at different shear rates (b) Effective emulsion viscosity compared with bitumen and water

Fig. 5—Calculated effective viscosities of oil-in-water emulsions at different shear rates at 35 bar and 373, 403, and 443 K. The viscosity of the 1,000 ppm brine is assumed to be the same as pure-water viscosity: 0.28, 0.21, and 0.16 cp at 373, 403, and 443 K, respectively. Bitumen viscosities are 205.6, 58.2, and 18.4 cp at 373, 403, and 443 K, respectively.

Temperature (K)	5 $seconds^{-1}$	10 $seconds^{-1}$	15 $seconds^{-1}$	29 $seconds^{-1}$
373	12.40	10.08	10.51	6.10
403	3.63	4.07	4.23	3.00
443	0.89	1.00	0.87	0.97

Table 2—Effective viscosities (cp) for emulsions at 373, 403, and 443 K and 35 bar at shear rates from 5 to 29 $seconds^{-1}$.

Analysis of Bitumen-Flow Rate in SAGD. Experimental data presented in this paper and Baek et al. (2018a) show that it is possible to form single-phase oil-in-water emulsions by adding DEA to mixtures of bitumen and brine. This subsection is concerned with how the bitumen transport by oil-in-water emulsion is compared with that by the two-phase flow of oil and water in conventional SAGD. To our knowledge, no reservoir simulator can represent DEA-SAGD with multicomponent, multiphase, thermal, reactive flow. Therefore, this issue is addressed by calculating the main factors affecting the molar flow rate of Athabasca bitumen under gravity drainage for assumed in-situ conditions beyond the edge of the steam chamber as follows:

- The pressure is 35 bar.
- The in-situ water/oil ratio is 7:3.
- NaCl-brine salinity is 1,000 ppm, which is higher than the usual salinity levels of produced water in SAGD.
- The DEA concentration in the aqueous solution is 0.5 wt%.

Although it is simple, this calculation mechanistically explains how the bitumen transport can be enhanced by oil-in-water emulsification.

Darcy's law applied to the edge of the steam chamber at elevation z gives

$$U_j(z) = -k_j \rho_j g \sin\theta / \mu_j = -k_j g \sin\theta / \upsilon_j, \quad (3)$$

where U_j is the Darcy flow velocity for an oil-containing phase j along the chamber edge, k_j is the effective permeability of phase j, and θ is the angle of the flow at elevation z. The symbols ρ_j, μ_j, and υ_j are mass density, viscosity, and kinematic viscosity of the oil-containing phase j, respectively. Integrating U_j for a cross section perpendicular to the edge of the steam chamber, the total flow rate of all oil-containing phases at elevation z is

$$q_o(z) = \int_0^{\xi_L} \sum_{j=1}^{N} U_j \Delta y \mathrm{d}\xi = -\int_0^{\xi_L} \sum_{j=1}^{N} (k_j g \sin\theta / \upsilon_j) \Delta y \mathrm{d}\xi = -kg\sin\theta \Delta y I_o, \quad (4)$$

where N is the total number of oil-containing phases and k is the absolute permeability assumed to be constant with ξ. The ξ direction is perpendicular to the steam chamber edge. $\xi = 0$ at the edge of the steam chamber. ξ_L is the distance from the steam-chamber edge where oil-containing-phase flow diminishes. Δy is the unit length along the horizontal section of an SAGD well pair. I_o is defined as

$$I_o(z) = \int_0^{\xi_L} \sum_{j=1}^{N} \frac{k_{rj}}{\upsilon_j} \mathrm{d}\xi. \quad \ldots\ldots (5)$$

The molar flow rate of the bitumen component in the oil-containing phases is then calculated as

$$q_{bo}(z) = -kg\sin\theta \Delta y I_{bo}, \quad \ldots\ldots (6)$$

where

$$I_{bo}(z) = \int_0^{\xi_L} \sum_{j=1}^{N} (k_{rj}\underline{\rho}_j x_{bj}/\upsilon_j)\mathrm{d}\xi. \quad \ldots\ldots (7)$$

In Eq. 7, k_{rj} is the relative permeability of the oil-containing phase j, $\underline{\rho}_j$ is the molar density of the oil-containing phase j, and x_{bj} is the molar concentration of the bitumen component in the oil-containing phase j. The integrand in Eq. 7 contains the influential parameters for bitumen transport. This integrand is calculated to explain the possible enhancement of bitumen transport by oil-in-water emulsification. For the calculation for DEA-SAGD, it is assumed that bitumen can be transported by a single phase of oil-in-water emulsion or by both oil-in-water emulsion and an excess oil phase. In the calculation for SAGD, it is assumed that bitumen is transported by the oleic phase that coexists with a separate condensed-water phase.

Eq. 4 was combined with local- and global-material-balance equations along with a 1D heat-conduction model and a linear chamber edge in Shi and Okuno (2018). However, to do so for emulsified bitumen requires more-comprehensive data for emulsion-phase behavior at a wide range of temperatures at a specified pressure, which are quite expensive to obtain and are beyond the scope of this paper. With the data obtained in this research, therefore, a comparison is made between the bitumen molar flow by oil-in-water emulsion and an excess oil phase, if present, in DEA-SAGD and that in the two-phase flow of oil and water in conventional SAGD in terms of the integrand of Eq. 7. This comparison is made on the basis of the phase-behavior data for the integrand at 373, 403, and 443 K at 35 bar. Note that the integrand accounts for the effective permeability of the phases that transport the bitumen component.

Mass densities and effective viscosities of the oil-in-water emulsion using DEA were obtained at 373, 403, and 443 K and 35 bar in this research. An average viscosity that represents the emulsion viscosity at each temperature was taken for the data for the shear rates between 5 and 10 seconds^{-1}. The molar density of the emulsion can be calculated as the measured mass density divided by the molecular weight.

For the SAGD counterpart, ideal mixing was assumed for the calculation of densities for brine/bitumen mixtures. Viscosities of bitumen at 373, 403, and 443 K and 35 bar are 205.6, 58.2, and 18.4 cp, and those for water are 0.28, 0.21, and 0.16 cp, respectively. Then, the viscosity of a water-containing oil phase was calculated using the SAGD liquid-viscosity model of Venkatramani and Okuno (2015). Properties of water are taken from the National Institute of Standards and Technology's database (NIST REFPREP, version 7). Properties of bitumen other than viscosities are from Baek et al. (2019a), who studied the same bitumen sample.

The molar compositions, phase identity, and phase saturations used for the molar-flow-rate calculation are summarized in **Table 3.** Phase-equilibrium calculations were performed at 35 bar and temperatures from 373 and 443 K to determine the oil-phase composition for the brine/bitumen mixture (with no DEA) according to the Peng-Robinson equation of state (PR-EOS) models by Venkatramani and Okuno (2015). To compare DEA-SAGD with SAGD, the same water/oil ratio (WOR) (7:3) is assumed. Corey's relative permeability models were assumed in the calculation:

$$k_{rw} = k_{rw}^{o}\left(\frac{S_w - S_{wr}}{1 - S_{wr} - S_{or}}\right)^n, \quad \ldots\ldots (8)$$

$$k_{ro} = k_{ro}^{o}\left(\frac{1 - S_w - S_{or}}{1 - S_{wr} - S_{or}}\right)^m, \quad \ldots\ldots (9)$$

where k_{rw} and k_{ro} are the relative permeabilities for water and oil phases. k_{rw}^{o} and k_{ro}^{o} are the endpoint relative permeabilities at irreducible water and oil saturations, respectively. S_w, S_{wr}, and S_{or} are water saturation, residual water saturation, and residual oil saturation, respectively. Exponents m and n determine the curvature of the relative permeabilities. The parameters for Corey's models for water-wet oil sands are given in **Table 4.** The corresponding relative permeability curves are shown in **Fig. 6.** Residual saturations were obtained from a case in Edmunds and Peterson (2007) corresponding to a steam/oil ratio of 2.3. Endpoint relative permeabilities of the water and oil phases for Corey's model were experimentally determined by Maini and Batycky (1985) for an oil-sand core in Canada. Sharma and Gates (2010) reported that the exponent m ranged from 2 to 4 on the basis of the SAGD field data of Canadian oil sands collected between 2005 and 2008. An averaged value, 2.7, for m was taken for the base case in this paper. The exponent n was obtained from the measurement of Polikar et al. (1990) for Athabasca oil sands. The same parameters for Corey's models are used in the calculation for both SAGD and DEA-SAGD at 443 K at which an emulsion phase and an excess oil phase coexist. The k_{rw} equation was assumed for the oil-in-water emulsion, and k_{ro} for the oil phase for DEA-SAGD at 443 K. **Table 5** gives the resulting relative permeabilities for bitumen-containing phases for SAGD and DEA-SAGD. Natural surfactants created in DEA-SAGD likely decrease the interfacial tension between the water and bitumen phases, but this possibility was not included in the calculation in this paper.

Fig. 7 shows the evaluation of the integrand in Eq. 7 for the SAGD case from 373 to 515 K and the DEA-SAGD case from 373 to 443 K at 35 bar. Table 5 presents the values of the integrand for each bitumen-containing phase in SAGD and DEA-SAGD. The integrand for the DEA-SAGD case is 345 times greater at 373 K, 273 times greater at 403 K, and 19 times greater at 443 K in comparison with that for the SAGD case. The integrand of the DEA-SAGD case from 373 to 443 K cannot be reached by the SAGD case even at the highest temperature, 515 K. At 443 K, the bitumen molar flow in the DEA case occurs through the oil-in-water-emulsion phase, although the bitumen content is small in the emulsion. This is a preliminary evaluation of the enhancement of in-situ bitumen transport by DEA-SAGD, but the results indicate that oil-in-water emulsification has a substantial potential for energy-efficient SAGD operations.

Influential factors in the integrand were analyzed to understand potential mechanisms for DEA-SAGD to increase in-situ bitumen transport. Fig. 7b compares the product of molar density and bitumen concentration for the bitumen-containing phases for SAGD and DEA-SAGD. This product can be viewed as the molarity of bitumen in a bitumen-containing phase. The bitumen molarity in oil-in-water emulsion is 0.3 times that of the oil phase in SAGD at 373 and 403 K. At 443 K, the bitumen molarity in oil-in-water emulsion is only 0.12 times that of the oil phase in SAGD.

Temperature (K)	Recovery Process	Water (mol%)	Bitumen (mol%)	Solvent (mol%)	Bitumen-Containing Phase Identity	Bitumen-Containing Phase Saturation
373	SAGD	3.6	96.4	–	Oil phase	0.300
	DEA-SAGD	98.4	1.5	0.1	Emulsion phase	1.000
403	SAGD	6.8	93.2	–	Oil phase	0.300
	DEA-SAGD	98.4	1.5	0.1	Emulsion phase	1.000
443	SAGD	13.6	86.4	–	Oil phase	0.300
	DEA-SAGD	83.8	16.2	0	Oil phase	0.253
		99.4	0.5	0.1	Emulsion phase	0.747

Table 3—Molar composition, phase identity, and phase saturation of the bitumen-containing phase in SAGD and DEA-SAGD in molar-flow-rate calculation. Compositions for oil phase in SAGD are obtained by phase-equilibrium calculation with Venkatramani and Okuno (2015) PR-EOS models. WOR in SAGD is assumed to be 7:3.

Parameters	Values (Fig. 6)
S_{wr}	0.15
S_{or}	0.15
k^o_{rw}	0.20
k^o_{ro}	1.00
m	2.7
n	3.5

Table 4—Parameters for Corey's relative permeability model as defined in Eqs. 8 and 9 (Maini and Batycky 1985; Polikar et al. 1990; Edmunds and Peterson 2007; Sharma and Gates 2010).

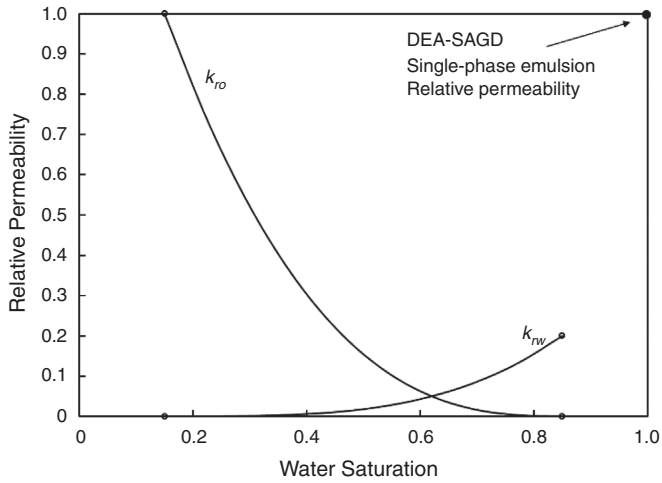

Fig. 6—Corey's relative permeability models for the calculation of bitumen molar flow rate with the integrand in Eq. 7 (Maini and Batycky 1985; Polikar et al. 1990; Edmunds and Peterson 2007; Sharma and Gates 2010).

Temperature (K)	Recovery Process	Bitumen-Containing Phase Identity	Relative Permeability	Integrand (10^3 mol·s·m^{-5})
373	SAGD	Oil phase	0.0156	136.6
	DEA-SAGD	Emulsion phase	1.0000	47 197.6
403	SAGD	Oil phase	0.0156	479.9
	DEA-SAGD	Emulsion phase	1.0000	130 985.0
443	SAGD	Oil phase	0.0156	1550.7
	DEA-SAGD	Oil phase	0.0057	7090.56
		Emulsion phase	0.1146	22 663.64

Table 5—Relative permeabilities and bitumen-molar-flow-rate calculation with the integrand of bitumen-containing phases in Eq. 7.

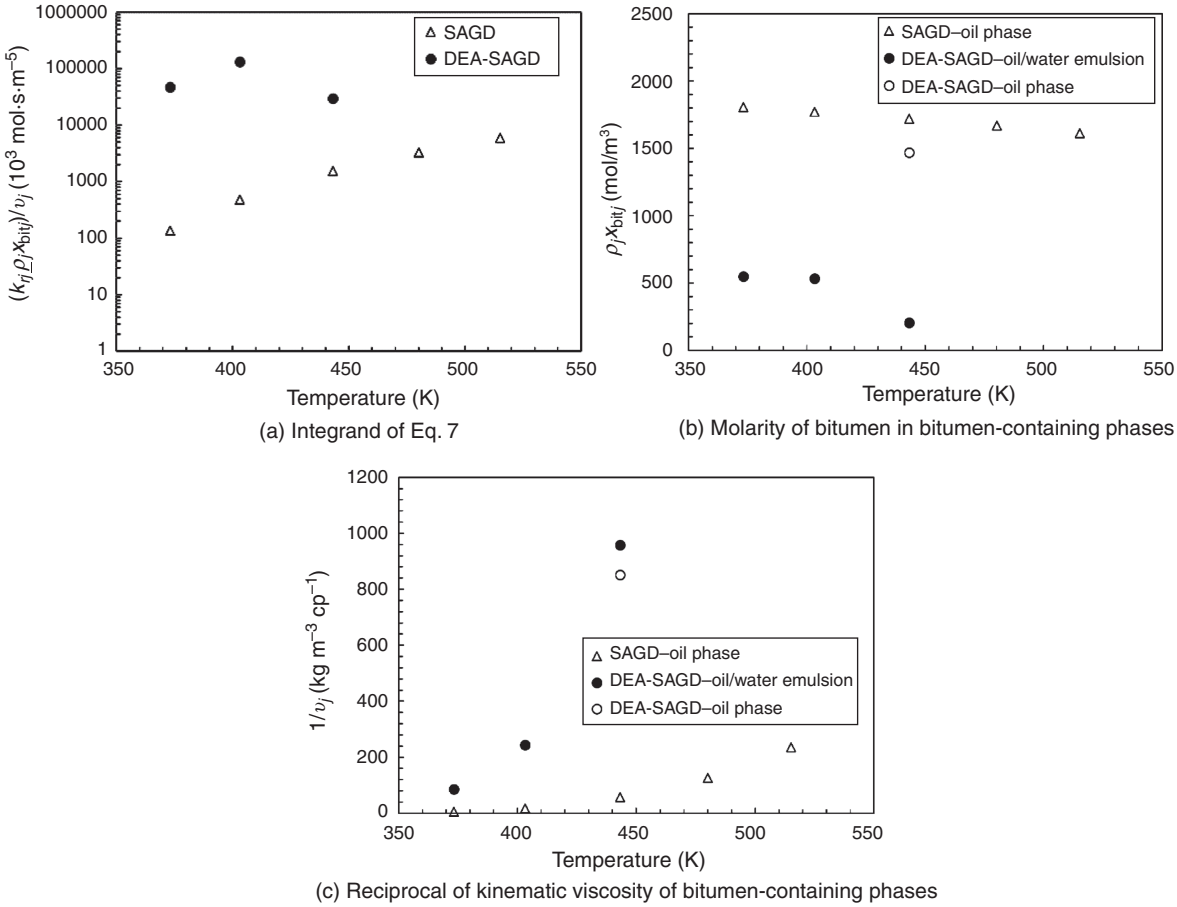

(a) Integrand of Eq. 7

(b) Molarity of bitumen in bitumen-containing phases

(c) Reciprocal of kinematic viscosity of bitumen-containing phases

Fig. 7—Bitumen-molar-flow-rate analysis with the integrand of Eq. 7, and bitumen molarity and kinematic viscosity of bitumen-containing phases at 35 bar and temperatures from 373 to 443 K for DEA-SAGD and up to 515 K for SAGD. An average is taken for emulsion viscosities at 5 and 10 seconds^{-1} for the viscosity used for the bitumen-molar-flow-rate calculation.

Although the emulsification of bitumen yields a fractional bitumen molarity, which is quite small at 443 K, the bitumen component can be transported in the water-external phase by adding only 0.12 mol% DEA. The effective permeability of the bitumen-containing phase for DEA-SAGD (i.e., the emulsion phase) is calculated to be 64 times greater than that of the bitumen-rich phase of SAGD (i.e., the oil phase) at 373 and 403 K. At 443 K, the oil-in-water-emulsion phase has an effective permeability that is 7 times greater than that of the oil phase of SAGD.

The capability of transporting bitumen can also be enhanced by lowering the kinematic viscosity of the bitumen-containing phase through oil-in-water emulsion. As shown in Fig. 7c, the reciprocals of kinematic viscosity for the emulsion are 18, 14, and 17 times greater than oil-phase viscosity in SAGD at 373, 403, and 443 K, respectively. This indicates that in terms of kinematic-viscosity reduction, emulsion kinematic viscosities at 373 and 403 K are equivalent to the oil phase in the SAGD case at 472 and 515 K, respectively.

This research was focused on oil-in-water-emulsion flow in a porous medium. Additional issues regarding the application of organic alkali to SAGD include the following: the condensation behavior of the coinjected organic alkali, the mixing of the condensed organic alkali with bitumen and water in a porous medium, the phase behavior of organic-alkali/bitumen/water mixtures, the effect of divalent cations and clays on bitumen emulsification, and the rheology and stability of bitumen-in-water emulsion in different porous media.

The highest temperature in this research was 443 K. This might be lower than the injected steam temperatures in SAGD operations. However, temperatures beyond the thermal fronts, where bitumen and condensed water flow, can be much lower than the injected steam temperatures (Birrell 2001; Gates and Larter 2014; Shi and Okuno 2018). Furthermore, the chamber-edge temperature in solvent-SAGD can be lower than that achieved by injecting steam alone. Previous phase-behavior and simulation studies indicated that C_6-steam coinjection at 35 bar might result in a chamber-edge temperature near 450 K, which is approximately 60 K lower than that by injecting steam alone (Dong 2012; Keshavarz et al. 2015; Venkatramani and Okuno 2018).

DEA was selected as the organic alkali in this research and in Baek et al. (2018a). However, Baek et al. (2019b) recently showed that pyrrolidine can be another promising organic alkali in terms of bitumen-in-water emulsification at a wide range of temperature. The phase behavior presented in this paper is obviously specific to DEA—i.e., different organic alkalis will give different phase-behavior results for the same bitumen. Likewise, bitumens with different acid numbers will result in different phase behavior for the same organic alkali used for emulsification.

Conclusions

DEA was studied as a potential additive to steam for improving the efficiency of SAGD. The oil-in-water emulsions studied were made by mixing an aqueous solution of 1,000 ppm NaCl and 0.5 wt% DEA with Athabasca bitumen at a volume ratio of 7:3. Then, phase behavior and effective viscosities of the emulsions were measured with an in-line density meter and a glass-bead-pack flow system at 35 bar and temperatures from 373 to 443 K. Bitumen molar flow rate in DEA-SAGD was compared with that in SAGD by use of Darcy's law for gravity drainage along with the new experimental data. Conclusions are as follows:

- At 35 bar and from 373 to 403 K, bitumen was totally emulsified into water by activating acidic components of the bitumen as natural surfactants. At 443 K, bitumen was partly emulsified into water and coexisted with an excess-oil phase.
- The emulsion showed weakly shear-thinning behavior at 373 K and 35 bar. At 403 and 443 K, the emulsion viscosity did not show a clear sensitivity to shear rate from 5 to 29 seconds^{-1}.
- In-situ bitumen transport can be enhanced by the emulsification of bitumen into water using DEA. The integrand in Eq. 7 is an indicator of the bitumen-flow capability in gravity drainage. The integrand for the emulsified bitumen was calculated to be 345, 273, and 19 times greater than that for SAGD with the overall DEA concentration of 0.12 mol% at 373, 403, and 443 K, respectively. Bitumen transport for the DEA-SAGD case from 373 to 443 K was calculated to be even more efficient than that for SAGD at 515 K.
- The enhanced mobility of bitumen by emulsification comes from the increased effective permeability of the emulsion phase that transports the bitumen component and the reduced kinematic viscosity. In-situ transport of bitumen as oil-in-water emulsion can be more efficient than the bitumen transport as the two-phase flow of oil and water in conventional SAGD, especially at relatively low temperatures (e.g., less than 403 K). At 443 K, only a fraction of bitumen is emulsified into water. However, the results showed that an emulsion that is lean in bitumen can still be an efficient bitumen carrier because of the large mobility of the water-external phase.

Nomenclature

g = gravitational constant, 9.8 m/s^2
I = parameter defined in Eq. 5
k = absolute permeability, darcies
k_r = relative permeability
m, n = parameters for Corey relative permeability models
P = pressure, bar
q = flow rate
S = saturation
U = Darcy flow velocity
x = mole fraction
y = length of reservoir parallel to well pair, m
z = elevation from the production well on the chamber edge, m
α = reservoir diffusivity, m^2/s
θ = angle between tangent to chamber edge and horizontal line
μ = dynamic viscosity, cp
ξ = distance from perpendicular to chamber edge, m
ρ = mass density, kg/m^3
$\underline{\rho}$ = molar density, mol/m^3
υ = kinematic viscosity, cp·m^3/kg

Subscripts

b = bitumen
j = oil-containing phase
L = mobilized bitumen
o = oil-containing phases
or = residual oil
w = water
wr = residual water

Superscript

o = end point

Acknowledgments

The authors gratefully acknowledge the financial support from Japan Canada Oil Sands Limited and the Chemical Enhanced Oil Recovery (EOR) Industrial Affiliates Project at the University of Texas at Austin. Ryosuke Okuno holds the Pioneer Corporation Faculty Fellowship in Petroleum Engineering at the University of Texas at Austin. The authors thank Gary A. Pope for sharing his equipment and also Glen S. Baum for his assistance with this research.

References

Baek, K. H., Argüelles-Vivas, F. J., Okuno, R. et al. 2018a. An Experimental Study of Emulsion Phase Behavior and Viscosity for Athabasca-Bitumen/Diethylamine/Brine Mixtures. *SPE Res Eval & Eng* **22** (2): 628–641. SPE-189768-PA. https://doi.org/10.2118/189768-PA.

Baek, K. H, Argüelles-Vivas, F. J., Okuno, R. et al. 2018b. Emulsification of Athabasca Bitumen by Organic Alkali: Emulsion Phase Behavior and Viscosity for Athabasca-Bitumen/Brine/Triethylenetetramine. *J Pet Sci Eng* **168:** 359–369. https://doi.org/10.1016/j.petrol.2018.04.063.

Baek, K., Sheng, K., Argüelles-Vivas, F. J. et al. 2019a. Comparative Study of Oil Dilution Capability of Dimethyl Ether and Hexane as Steam Additives for SAGD. *SPE Res Eval & Eng* **22** (3): 1030–1048. SPE-187182-PA. https://doi.org/10.2118/187182-PA.

Baek, K. H., Okuno, R., Sharma, H. et al. 2019b. Oil-in-Water Emulsification of Athabasca Bitumen with Pyrrolidine Solution. *Fuel* **246:** 425–442. https://doi.org/10.1016/j.fuel.2019.02.123.

Birrell, G. E. 2001. Heat Transfer Ahead of a SAGD Steam Chamber, A Study of Thermocouple Data from Phase B of the Underground Test Facility (Dover Project). Paper presented at the SPE Annual Technical Conference and Exhibition, New Orleans, Louisiana, USA, 30 September–3 October. SPE-71503-MS. https://doi.org/10.2118/71503-MS.

Bryan, J. and Kantzas, A. 2007a. Potential for Alkali-Surfactant Flooding in Heavy Oil Reservoirs Through Oil-in-Water Emulsification. Paper presented at the Canadian International Petroleum Conference, Calgary, Alberta, Canada, 12–14 June. PETSOC-09-02-37. https://doi.org/10.2118/09-02-37.

Bryan, J. and Kantzas, A. 2007b. Enhanced Heavy-Oil Recovery by Alkali-Surfactant Flooding. Paper presented at the SPE Annual Technical Conference and Exhibition, Anaheim, California, USA, 11–14 November. SPE-110738-MS. https://doi.org/10.2118/110738-MS.

Bryan, J., Mai, A., and Kantzas, A. 2008. Investigation into the Processes Responsible for Heavy Oil Recovery by Alkali-Surfactant Flooding. Paper presented at the SPE Symposium on Improved Oil Recovery, Tulsa, Oklahoma, USA, 20–23 April. SPE-113993-MS. https://doi.org/10.2118/113993-MS.

Dong, M., Ma, S., and Liu, Q. 2009. Enhanced Heavy Oil Recovery Through Interfacial Instability: A Study of Chemical Flooding for Brintnell Heavy Oil. *Fuel* **88:** 1049–1056. https://doi.org/10.1016/j.fuel.2008.11.014.

Dong, L. 2012. Effect of Vapour–Liquid Phase Behaviour of Steam–Light Hydrocarbon Systems on Steam Assisted Gravity Drainage Process for Bitumen Recovery. *Fuel* **95:** 159–168. https://doi.org/10.1016/j.fuel.2011.10.044.

Edmunds, N. and Peterson, J. 2007. A Unified Model for Prediction of CSOR in Steam-Based Bitumen Recovery. Paper presented at the Canadian International Petroleum Conference, Calgary, Alberta, Canada, 12–14 June. PETSOC-2007-027. https://doi.org/10.2118/2007-027.

Fan, T. and Buckley, J. 2007. Acid Number Measurements Revisited. *SPE J.* **12** (4): 496–500. SPE-99884-PA. https://doi.org/10.2118/99884-PA.

Fortenberry, R., Kim, D., Nizamidin, N. et al. 2015. Use of Cosolvents to Improve Alkaline/Polymer Flooding. *SPE J.* **20** (2): 255–266. SPE-166478-PA. https://doi.org/10.2118/166478-PA.

Gates, I. D. 2007. Oil Phase Viscosity Behavior in Expanding-Solvent Steam-Assisted Gravity Drainage. *J Pet Sci Eng* **59** (1–2): 123–134. https://doi.org/10.1016/j.petrol.2007.03.006.

Gates, I. D. and Larter, S. R. 2014. Energy Efficiency and Emissions Intensity of SAGD. *Fuel* **115:** 706–713. https://doi.org/10.1016/j.fuel.2013.07.073.

Gupta, S., Gittins, S., and Picherack, P. 2005. Field Implementation of Solvent Aided Process. *J Can Pet Technol* **44** (11): 8–13. PETSOC-05-11-TN1. https://doi.org/10.2118/05-11-TN1.

Gupta, S. C. and Gittins, S. D. 2006. Christina Lake Solvent Aided Process Pilot. *J Can Pet Technol* **45** (9): 15–18. PETSOC-2005-190. https://doi.org/10.2118/2005-190.

Haddadnia, A., Azinfar, B., Zirrahi, M. et al. 2018. Thermophysical Properties of Dimethyl Ether/Athabasca Bitumen System. *Can J Chem Eng* **96:** 597–604. https://doi.org/10.1002/cjce.23009

Ivory, J. J., Zheng, R., Nasr, T. N. et al. 2008. Investigation of Low Pressure ES-SAGD. Paper presented at the SPE International Thermal Operations and Heavy Oil Symposium, Calgary, Alberta, Canada, 20–23 October. SPE-117759-MS. https://doi.org/10.2118/117759-MS.

Keshavarz, M., Okuno, R., and Babadagli, T. 2014. Efficient Oil Displacement Near the Chamber Edge in ES-SAGD. *J Pet Sci Eng* **118:** 99–113. https://doi.org/10.1016/j.petrol.2014.04.007.

Keshavarz, M., Okuno, R., and Babadagli, T. 2015. Optimal Application Conditions for Steam/Solvent Coinjection. *SPE Res Eval & Eng* **18** (1): 20–38. SPE-165471-PA. https://doi.org/10.2118/165471-PA.

Kim, M., Abedin, A., Lele, P. et al. 2017. Microfluidic Pore-Scale Comparison of Alcohol- and Alkaline-Based SAGD Processes. *J Pet Sci. Eng.* **154:** 139–149. https://doi.org/10.1016/j.petrol.2017.04.025.

Kumar, R., Dao, E., and Mohanty, K. 2012. Heavy-Oil Recovery by In-Situ Emulsion Formation. *SPE J.* **17** (2): 326–334. SPE-129914-PA. https://doi.org/10.2118/129914-PA.

Lake, L. W., Johns, R., Rossen, W. R. et al. 2014. *Fundamentals of Enhanced Oil Recovery*. Richardson, Texas, USA: Society of Petroleum Engineers.

Leaute, R. P. 2002. Liquid Addition to Steam for Enhancing Recovery (LASER) of Bitumen with CSS: Evolution of Technology from Research Concept to a Field Pilot at Cold Lake. Paper presented at the SPE International Thermal Operations and Heavy Oil Symposium and International Horizontal Well Technology Conference, Calgary, Alberta, Canada, 4–7 November. SPE-79011-MS. https://doi.org/10.2118/79011-MS.

Leaute, R. P. and Carey, B. S. 2007. Liquid Addition to Steam for Enhancing Recovery (LASER) of Bitumen with CSS: Results from the First Pilot Cycle. *J Can Pet Technol* **46** (9): 22–30. PETSOC-07-09-01. https://doi.org/10.2118/07-09-01.

Li, W., Mamora, D. D., and Li, Y. 2011a. Light-and Heavy-Solvent Impacts on Solvent-Aided-SAGD Process: A Low-Pressure Experimental Study. *J Can Pet Technol* **50** (4): 19–30. SPE-133277-PA. https://doi.org/10.2118/133277-PA.

Li, W., Mamora, D. D., and Li, Y. 2011b. Solvent-Type and -Ratio Impacts on Solvent-Aided SAGD Process. *SPE Res Eval & Eng* **14** (3): 320–331. SPE-130802-PA. https://doi.org/10.2118/130802-PA.

Liu, Q., Dong, M., Ma, S. et al. 2007. Surfactant Enhanced Alkaline Flooding for Western Canadian Heavy Oil Recovery. *Colloids Surf A Physicochem Eng Asp* **293:** 63–71. https://doi.org/10.1016/j.colsurfa.2006.07.013.

Liu, Q., Dong, M., Yue, X. et al. 2006. Synergy of Alkali and Surfactant in Emulsification of Heavy Oil in Brine. *Colloids Surf A Physicochem Eng Asp* **273:** 219–228. https://doi.org/10.1016/j.colsurfa.2005.10.016.

Lu, C., Liu, H., Zhao, W. et al. 2017. Experimental Investigation of In-Situ Emulsion Formation to Improve Viscous-Oil Recovery in Steam-Injection Process Assisted by Viscosity Reducer. *SPE J.* **22** (1): 130–137. SPE-181759-PA. https://doi.org/10.2118/181759-PA.

Maini, B. B. and Batycky, J. P. 1985. Effect of Temperature on Heavy-Oil/Water Relative Permeabilities in Horizontally and Vertically Drilled Core Plugs. *J Pet Technol* **37** (8): 1500–1510. SPE-12115-PA. https://doi.org/10.2118/12115-PA.

Meng, L., Ji, D., Dong, M. et al. 2018. Experimental and Numerical Study of the Convective Mass Transfer of Solvent in the Expanding-Solvent SAGD Process. *Fuel* **215:** 298–311. https://doi.org/10.1016/j.fuel.2017.11.028.

Mohammadmoradi, P., Taheri, S., and Kantzas, A. 2017. Interfacial Areas in Athabasca Oil Sands. *Energy Fuels* **31** (8): 8131–8145. https://doi.org/10.1021/acs.energyfuels.7b01458.

Mohebati, M. H., Maini, B. B., and Harding, T. G. 2012. Numerical-Simulation Investigation of the Effect of Heavy-Oil Viscosity on the Performance of Hydrocarbon Additives in SAGD. *SPE Res Eval & Eng* **15** (2): 165–181. SPE-138151-PA. https://doi.org/10.2118/138151-PA.

Nasr, T. N., Beaulieu, G., Golbeck, H. et al. 2003. Novel Expanding Solvent-SAGD Process "ES-SAGD". *J Can Pet Technol* **42** (1): 13–16. PETSOC-03-01-TN. https://doi.org/10.2118/03-01-TN.

Pei, H., Zhang, G., Ge, J. et al. 2013. Potential of Alkaline Flooding to Enhance Heavy Oil Recovery Through Water-in-Oil Emulsification. *Fuel* **104:** 284–293. https://doi.org/10.1016/j.fuel.2012.08.024.

Polikar, M., Ali, S. M., and Puttagunta, V. R. 1990. High-Temperature Relative Permeabilities for Athabasca Oil Sands. *SPE Res Eval & Eng* **5** (1): 25–32. SPE-17424-PA. https://doi.org/10.2118/17424-PA.

Sadowski, T. J. and Bird, R. B. 1965. Non-Newtonian Flow Through Porous Media—I: Theoretical. *J Rheol* **9** (2): 243–250. https://doi.org/10.1122/1.549000.

Sharma, J. and Gates, I. D. 2010. Multiphase Flow at the Edge of a Steam Chamber. *Can J Chem Eng* **88** (3): 312–321. https://doi.org/10.1002/cjce.20280.

Shen, C. 2013. *Enhanced Oil Recovery Field Case Studies*, first edition, Chap. 13, 413–455. Waltham, Massachusetts, USA: Gulf Professional Publishing.

Sheng, K., Okuno, R., and Wang, M. 2018. Dimethyl Ether as an Additive to Steam for Improved Steam-Assisted Gravity Drainage. *SPE J.* **23** (4): 1201–1222. SPE-184983-PA. https://doi.org/10.2118/184983-PA.

Shi, X. and Okuno, R. 2018. Analytical Solution for Steam-Assisted Gravity Drainage with Consideration of Temperature Variation Along the Edge of a Steam Chamber. *Fuel* **217:** 262–274. https://doi.org/10.1016/j.fuel.2017.12.110.

Srivastava, P. and Castro, L. 2011. Successful Field Application of Surfactant Additives to Enhance Thermal Recovery of Heavy Oil. Paper presented at the SPE Middle East Oil and Gas Show and Conference, Manama, Bahrain, 25–28 September. SPE-140180-MS. https://doi.org/10.2118/140180-MS.

Venkatramani, A. and Okuno, R. 2015. Characterization of Water-Containing Reservoir Oil Using an EOS for Steam Injection Processes. *J Natural Gas Sci Eng* **26:** 1091–1106. https://doi.org/10.1016/j.jngse.2015.07.036.

Venkatramani, A. and Okuno, R. 2018. Mechanistic Simulation Study of Expanding-Solvent Steam-Assisted Gravity Drainage Under Reservoir Heterogeneity. *J Pet Sci Eng* **169:** 146–156. https://doi.org/10.1016/j.petrol.2018.04.074.

Xiao, R., Teletzke, G., Lin, M. et al. 2017. A Novel Mechanism of Alkaline Flooding to Improve Sweep Efficiency for Viscous Oils. Paper presented at the SPE Annual Technical Conference and Exhibition, San Antonio, Texas, USA, 9–11 October. SPE-187366-MS. https://doi.org/10.2118/187366-MS.

Zeidani, K. and Gupta, S. 2013. Surfactant-Steam Process: An Innovative Enhanced Heavy Oil Recovery Method for Thermal Applications. Paper presented at the SPE Heavy Oil Conference-Canada, Calgary, Alberta, Canada, 11–13 June. SPE-165545-MS. https://doi.org/10.2118/165545-MS.

Kai Sheng is a PhD-degree candidate in petroleum engineering in the Hildebrand Department of Petroleum and Geosystems Engineering at the University of Texas at Austin. His research interests include thermal EOR, numerical reservoir simulation, multiphase behavior, and fluid properties of heavy oil and bitumen. Sheng holds a BE degree from the China University of Petroleum (East China) and an MS degree from the University of Alberta, both in petroleum engineering. He is a member of SPE.

Francisco J. Argüelles-Vivas is a post-doctoral-degree fellow in the Hildebrand Department of Petroleum and Geosystems Engineering at the University of Texas at Austin, having previously worked as a reservoir engineer at the Mexican Petroleum Institute for 2 years. His current research interests are EOR methods for conventional/unconventional reservoirs, formation damage, phase behavior of mixtures of solvent and bitumen/heavy oil, pore-scale modeling, and carbon dioxide sequestration. Argüelles-Vivas holds a bachelor's degree in chemical engineering from the Metropolitan Autonomous University, Mexico; a master's degree in petroleum engineering from the Mexican Petroleum Institute; and a PhD degree in petroleum engineering from the University of Alberta. He is a member of SPE and currently serves as a technical reviewer for *SPE Journal*.

Kwang Hoon Baek is a PhD-degree candidate in petroleum engineering in the Hildebrand Department of Petroleum and Geosystems Engineering at the University of Texas at Austin. His research interests include thermal EOR, chemical EOR, multiphase behavior, and fluid properties of petroleum fluids. Baek holds a bachelor's degree in chemical engineering from Yonsei University (South Korea) and a master's degree in science and technology policy from Korea Advanced Institute of Science and Technology. He is a member of SPE.

Ryosuke Okuno is an associate professor in the Hildebrand Department of Petroleum and Geosystems Engineering at the University of Texas at Austin. Before joining the faculty of his current department, he served as an assistant professor of petroleum engineering in the Department of Civil and Environmental Engineering at the University of Alberta from 2010 to 2015. Okuno also has 7 years of industrial experience as a reservoir engineer with Japan Petroleum Exploration Co. Ltd., and is a registered professional engineer in Alberta, Canada. His research and teaching interests include EOR, thermal oil recovery, unconventional oil and gas, numerical reservoir simulation, thermodynamics, multiphase behavior, and applied mathematics. Okuno is a recipient of the 2012 SPE Petroleum Engineering Junior Faculty Research Initiation Award and the 2019 SPE Regional Reservoir Description and Dynamics Award (Southwestern Region). He currently serves as an associate editor for *SPE Journal* and holds the Pioneer Corporation Faculty Fellowship in petroleum engineering at the University of Texas at Austin. Okuno holds bachelor's and master's degrees in geosystems engineering from the University of Tokyo, and a PhD degree in petroleum engineering from the University of Texas at Austin.